

Optical spectrum of a Hubbard chain

Pierre F. Maldague

IBM Thomas J. Watson Research Center, Yorktown Heights, New York 10598

(Received 18 April 1977)

The optical absorption of the one-dimensional Hubbard model is calculated by three different methods. Linear chains of five atoms and rings of five and seven atoms containing four electrons are treated numerically. The infinite-chain problem is solved first in the t -matrix approximation of Lyo and Holstein. It is shown that in this approximation, most of the high-frequency absorption is due to a bound state which lies above the band continuum. Finally, the absorption is evaluated in the memory-function formalism of Götze and Wölfle, which reduces to ordinary perturbation theory at high frequency. The three approaches are in qualitative agreement, and the differences between them can be explained by the nature of the approximations involved. Applications to tetrathiafulvalene-tetracyanoquinodimethane (TTF-TCNQ) and the platinum salt $K_2Pt(CN)_4Br_{0.3} \cdot 3H_2O$ (KCP) are discussed.

I. INTRODUCTION

The goal of this paper is to calculate the optical absorption of a one-dimensional, interacting system of electrons. Our work was motivated by the infrared and optical anomalies recently observed in the quasi-one-dimensional metals tetrathiafulvalene-tetracyanoquinodimethane (TTF-TCNQ) and $K_2Pt(CN)_4Br_{0.3} \cdot 3H_2O$ (KCP). It has been suggested by Torrance *et al.*¹ that the optical spectra of many TCNQ salts could be interpreted in terms of a strongly correlated Hubbard model, in which the long-range part of the Coulomb interaction is neglected. An unexplained anomaly has also been found² near the plasma edge of KCP; although it could plausibly be attributed to interband transitions,³ the possibility that the electron-electron interaction plays a role in these anomalies cannot be discarded. Such experiments point out the need for a reliable theory of optical-absorption processes in correlated one-dimensional systems. In the present paper, we discuss three different methods to calculate the absorption spectrum of the Hubbard model. The first method consists in calculating the spectra of finite chains numerically; this brute-force approach can only be used for relatively short chains. The second method is based on the t -matrix approximation introduced by Lyo and Holstein,^{4,5} who used it to calculate the low-frequency conductivity of the Hubbard model. We find that, in this approximation, most of the absorption is due to a bound state which lies above the band continuum, and which was neglected in their calculation (which is justified in the low-frequency limit considered by these authors). Finally, we calculate the optical conductivity in the memory-function approximation of Götze and Wölfle.⁶ This approach is exact in the weak-coupling limit, since it reduces to ordinary perturbation theory at high frequency. Our purpose in using this last approach

is twofold. First, it provides a test for the validity of the t -matrix approach in the weak-coupling limit. Second, it allows us to check the accuracy of the memory-function approximation when extrapolated to higher values of the coupling. We find that although the result of such an extrapolation has the correct order of magnitude, the memory-function approximation cannot be trusted for couplings which are not very weak. The failure of this approximation is related to that of the first Born approximation in the two-body scattering problem.

Three basic conclusions can be drawn from our results. First, the remarkable agreement between the numerical spectra and the t -matrix results indicates that the optical conductivity is indeed a measure of short-range correlations, which are correctly treated in the t -matrix approximation. This suggests that a similar method could also be used to treat more realistic models of a quasi-one-dimensional conductor. Second, we propose that the validity of the first Born approximation in a one- or two-body problem provides a useful criterion for the applicability of the memory-function approximation to the corresponding many-body problem. Third, we do find an absorption peak at a frequency of order U , the on-site repulsion energy, as suggested by Torrance *et al.* This peak is due to transitions in which the final state contains two electrons sitting at the same site. However, if we use parameters appropriate for TTF-TCNQ and KCP, we find that the optical (and infrared) absorption is quite small; most of the absorption occurs at or near zero frequency. This is especially true for KCP, which has a low carrier density (0.3 hole per Pt atom). Thus, it seems that some of the correlation effects neglected by the Hubbard model must play an important role in the optical anomalies observed in real quasi-one-dimensional conductors. This is hardly surprising, since the Hubbard model assumes (i) one tight-binding band, (ii)

a short-range interaction, and (iii) no electron-phonon interaction. On the other hand, our results do not imply that the correlation effects included in the Hubbard model are negligible; we only show that these effects do not *by themselves* explain the observed anomalies.

In the Hubbard approximation, the electron-electron interaction is represented by a term $\sum_i U \hat{n}_{i\uparrow} \hat{n}_{i\downarrow}$ in the Hamiltonian; U is the repulsion energy experienced by two electrons of opposite spin sitting at the same site i . *A priori*, one expects to see large effects in the conductivity if U is comparable to the half-bandwidth ϵ_0 . The magnitude of U has been estimated at ~ 0.3 eV in NMP-TCNQ,⁷ which is comparable to the bandwidth in TCNQ compounds. U has been calculated for two electrons on a transition metal atom,⁸ and found to be in the range 2–4 eV; this is somewhat less than the estimated bandwidth of KCP. These rough estimates clearly indicate that both KCP and TTF-TCNQ are strongly coupled systems.

The Hamiltonian for the one-dimensional Hubbard model is

$$\hat{H} = -\frac{\epsilon_0}{2} \sum_{i,\sigma} (\hat{a}_{i,\sigma}^\dagger \hat{a}_{i+1,\sigma} + \hat{a}_{i,\sigma}^\dagger \hat{a}_{i-1,\sigma}) + U \sum_i \hat{n}_{i\uparrow} \hat{n}_{i\downarrow}, \quad (1)$$

where $\hat{a}_{i\sigma}^\dagger$ creates an electron with spin σ at site i , $\hat{n}_{i\sigma} = \hat{a}_{i\sigma}^\dagger \hat{a}_{i\sigma}$ and $2\epsilon_0$ is the bandwidth. The two basic parameters of the theory are c , the average number of electrons per site, and $\mu = U/\epsilon_0$, which measures the strength of the interaction. The low-energy excitations of the interacting one-dimensional electron gas have been discussed extensively in the literature. In particular, exactly soluble models yield correlation functions exhibiting power-law singularities in the limit $\omega, q \rightarrow 0$.⁹ Such results have been used to discredit perturbative treatments, in which the power-law behavior manifests itself through logarithmic (infrared) singularities.¹⁰ Exact methods, however, rely on the Luttinger Hamiltonian,¹¹ which is characterized by an infinite bandwidth and a linear dispersion relation. While such simplifications of the band structure may not qualitatively affect the low-frequency behavior of the correlation functions, it will be apparent from our results that the finite bandwidth associated with the tight-binding Hamiltonian (1) plays an important role in optical absorption. It is therefore necessary to avoid the simplifications inherent in the Luttinger model, and to use some form of perturbation theory—which raises the specter of logarithmic divergences. There are two reasons, however, why we think that perturbation theory may give better results for the ($q=0$) conductivity than for other quantities such as the $2k_F$ electrical susceptibility. First of all, in the high-frequency

limit ($\omega \sim \epsilon_0$) the correlation functions should measure short-range rather than long-range correlations, and one therefore expects that an adequate theory of the optical absorption can be obtained if only short-range correlations are included—which is easily achieved in approximate theories. The second reason is that logarithmic singularities actually disappear from the perturbation-theoretic expression of the conductivity, at least in the simple approximation discussed in this paper. Loosely speaking, the low-energy excitations of the system contribute to normal electron-electron scattering processes, which do not affect the electrical current and do not contribute to the resistivity. The finite-frequency absorption is mainly due to Umklapp processes. In non-half-filled systems, such processes are inelastic and involve high-energy excitations to which a perturbative treatment may be applicable.

We can make the above remarks more precise by looking at the kinematics of electron-electron scattering in one dimension. In a noninteracting system, the crystal momentum k is conserved and there is no optical absorption. In the presence of interactions, a pair of electrons in a state $|k_i, k_i'\rangle$ can be scattered into a state $|k_f, k_f'\rangle$, thereby contributing to the absorption if the initial and final values of the current are different. In the low-frequency limit $\omega \ll \epsilon_0$, one can restrict oneself to elastic collisions. For given transfers of energy ω and crystal momentum q , there are only two possibilities for the initial and final electron states. In the first of these, $k_i' = k_f$ and $k_f' = k_i$; this is a normal process which leaves the total current unchanged. The second possibility is illustrated in Fig. 1. It corresponds to an Umklapp process, in which $k_i' = -\pi/a - k_i$ and $k_f' = \pi/a - k_f$, where a is the lattice constant. In this case, the value of the current does change. However, this process requires that one electron should initially lie in the top half of the band. For systems which are less than half filled ($c < 1$), this is very unlikely except at high

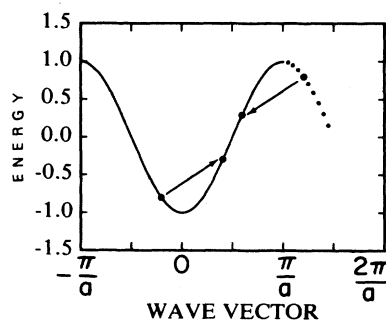


FIG. 1. Energy-wave-vector diagram for a one-dimensional elastic collision. Energy is in units of ϵ_0 .

temperature, when the logarithmic divergences of perturbation theory disappear anyway. It follows, then, that for temperatures and frequencies much less than the bandwidth, collisions cannot effectively degrade an electrical current, and the conductivity should look free-carrier-like. A similar reasoning applies to the case $c > 1$.

The above argument breaks down in a strongly correlated system, in which the interaction can excite many electrons out of the Fermi sea. In spite of this, our conclusion about the low-frequency behavior of the conductivity does apply to the limit $U \rightarrow \infty$, in which the system becomes equivalent to a noninteracting, spinless fermion gas. In this limit, all of the absorption is concentrated at $\omega = 0$, and the optical absorption vanishes. It is only in the intermediate coupling regime $U \sim \epsilon_0$ that one would expect to see some structure in the low-frequency conductivity.

In Sec. II, we present the general formalism and discuss our numerical spectra. Section III is devoted to the t -matrix approximation. Although this is a low-density approximation, we find that it gives good results even for nearly half-filled systems. In Sec. IV, we discuss the memory function approximation for $\sigma(\omega)$, which reduces to straightforward perturbation theory at high frequency. The good overall agreement between the three approaches gives us confidence that our approximate analysis provides an essentially correct description of the optical spectrum of the infinite Hubbard chain. Of course, our approach breaks down at low frequency, where the detailed structure of the low-lying excitations plays an important role. However, the existence of an exact sum rule for the conductivity of the Hubbard model allows us to indirectly determine the contribution of the zero-frequency absorption peak to the sum rule, which is sufficient for our purposes.

II. FINITE CHAINS AND NUMERICAL RESULTS

This section is devoted to the theory of the optical absorption in a finite chain of N "atoms" or sites. The motivation for the numerical work described later in this section is based on the assumption that the absorption spectra of such finite chains resemble the spectra of infinite chains having the same electron density. There can be no doubt that this is indeed true for large values of N (say, $N = 10^6$). The question is, then, how large an N should be chosen for the assumption to be valid. In principle, this could be checked by calculating the spectra of larger and larger chains, keeping the electron density approximately constant. Unfortunately, the dimension of the Hilbert space grows exponentially with N . Since a knowledge of all the

excited states is necessary to describe the spectrum of a chain, one quickly runs into formidable numerical difficulties even for $N \sim 10$. In fact, the numerical results reported here were obtained for only four electrons distributed over up to seven sites. While slightly larger "molecules" could certainly be handled as well, we found that the numerical spectra were in good qualitative agreement with the approximate theories which we developed to treat infinite chains. In particular, all the features of the numerical spectra can be interpreted in terms of physical processes that were included in the approximate treatments. Since the same physical processes are at work in larger chains, it is reasonable to assume that our results reflect the intrinsic properties of the Hubbard model rather than spurious size effects.

For simplicity, we first consider the case of a long chain, in which boundary effects can be neglected. This will enable us to introduce periodic boundary conditions, thereby simplifying the theoretical analysis. In the presence of an oscillating, uniform electric field $Ee^{-i\omega t}$ parallel to the chain, one must add to the Hamiltonian (1) a term representing the coupling to the applied field. This is conveniently done by introducing a vector potential $A(t) = cE/(-i\omega)e^{-i\omega t}$ into the Hamiltonian. Here and in the next two equations, c denotes the speed of light; this is not to be confused with the number of electrons per site, also denoted by c . Some care is needed to preserve gauge invariance in a tight-binding system; if x_i is the position of the i th atom in the chain, then a canonical transformation $\hat{a}'_i = e^{-i(e/c)Ax_i}\hat{a}_i$ should remove the coupling to a static vector potential A . This indicates that in the presence of a time-dependent vector potential $A(t)$, the first term in the Hamiltonian (1) becomes ($\hbar = 1$)

$$\hat{H}'_0 = -\frac{\epsilon_0}{2} \sum_{i,\sigma} (\hat{a}'_{i,\sigma} \hat{a}_{i+1,\sigma} e^{-ieaA(t)/c} + \hat{a}'_{i,\sigma} \hat{a}_{i-1,\sigma} e^{ieaA(t)/c}), \quad (2)$$

where a is the lattice constant. Expanding to second order in A , we find that the coupling term is

$$\hat{H}_A = (A/c)\hat{j} + \frac{1}{2}(e/c)^2 A^2 a^2 (-\hat{H}_0), \quad (3)$$

where \hat{H}_0 is the kinetic energy, i.e., the first term in the Hamiltonian (1) and \hat{j} is the current operator

$$\hat{j} = iea \frac{\epsilon_0}{2} \sum_{i,\sigma} (\hat{a}'_{i,\sigma} \hat{a}_{i+1,\sigma} - \hat{a}'_{i,\sigma} \hat{a}_{i-1,\sigma}). \quad (4)$$

We will base our discussion on the fluctuation-dissipation theorem, which relates the conductivity to the equilibrium current-current correlation function χ :

$$\sigma(\omega) = [\chi(\omega) - ne^2/m^*]/i\omega, \quad (5)$$

where $n = cN$ is the number of electrons and m^* is

an effective mass given by¹²

$$1/m^* = -a^2 \langle \hat{H}_0 \rangle / n. \quad (6)$$

In the dilute limit, electrons lie near the bottom of the band, and $1/m^* = a^2 \epsilon_0$. More generally, in a noninteracting system, one finds $1/m^* = a^2 \epsilon_0 (\sin \pi c / 2) / (\pi c / 2)$. The retarded correlation function χ is defined by

$$\chi(\omega) = i \int_0^\infty dt e^{i\omega t} \langle [\hat{j}(t), \hat{j}(0)] \rangle. \quad (7)$$

In terms of plane wave states, the current \hat{j} is given by

$$\hat{j} = -e \sum_{k, \sigma} \hat{a}_{k, \sigma}^\dagger \hat{a}_{k, \sigma} v_k, \quad v_k = a \epsilon_0 \sin ka, \quad (8)$$

where k is the (one-dimensional) wave vector, and a is the lattice constant.

Later on in this article, we will use approximations whose validity is restricted to high frequencies. To obtain information about the low-frequency conductivity, we will use the analog of the f -sum rule for a tight-binding system:

$$\frac{2}{\pi} \int_0^\infty \sigma'(\omega) d\omega = ne^2 / m^*, \quad (9)$$

where σ' denotes the real part of the conductivity and m^* is the effective mass defined in Eq. (6).

Before proving the sum rule, let us consider in some detail the case of a finite chain. The site indices in the Hamiltonian (1) are now restricted by the condition $1 \leq i \leq N$. If we denote by $|n\rangle$ and E_n the exact eigenstates and energy levels of the many-body Hamiltonian (1), the current-current correlation function (7) becomes

$$\chi(\omega) = \sum_n |\langle 0 | \hat{j} | n \rangle|^2 \left(\frac{1}{\omega + E_n - E_0 - i\eta} - \frac{1}{\omega - E_n + E_0 + i\eta} \right), \quad (10)$$

where $|0\rangle$ and E_0 denote the ground state and the ground-state energy, respectively. From Eq. (5), the real part of the conductivity is

$$\sigma'(\omega) = \pi \sum_n |\langle 0 | \hat{j} | n \rangle|^2 \frac{\delta(|\omega| - E_n + E_0)}{E_n - E_0}. \quad (11)$$

Thus, the spectrum of a finite chain consists of a series of sharp lines corresponding to transitions from the ground state to the excited states. When N is large, these lines merge into a continuum and σ is a continuous function of the frequency. To compare the spectra of finite and infinite chains, it is convenient to introduce the normalized integrated conductivity $Z(\omega)$, defined by

$$\begin{aligned} Z(\omega) &= \frac{2m^*}{\pi n e^2} \int_0^\omega d\nu \sigma'(\nu), \\ &= \frac{m^*}{n} \sum_{E_n - E_0 < \omega} \frac{|\langle 0 | \hat{v} | n \rangle|^2}{E_n - E_0}, \end{aligned} \quad (12)$$

where \hat{v} is the velocity operator $-\hat{j}/e$. Clearly, the sum rule implies that $Z \rightarrow 1$ as $\omega \rightarrow \infty$. To prove the sum rule, we observe that the current operator satisfies the equation

$$\hat{j} = ie[\hat{x}, \hat{H}], \quad (13)$$

where \hat{x} is the sum of the position operators of the electrons. Therefore,

$$\langle 0 | \hat{j} | n \rangle = ie(E_n - E_0) \langle 0 | \hat{x} | n \rangle; \quad (14)$$

inserting this into Eq. (11), we find

$$\begin{aligned} \frac{2}{\pi} \int_0^\infty \sigma'(\omega) d\omega &= ie \sum_n (\langle 0 | \hat{x} | n \rangle \langle n | \hat{j} | 0 \rangle \\ &\quad - \langle 0 | \hat{j} | n \rangle \langle n | \hat{x} | 0 \rangle), \quad (15) \\ &= -ie \langle 0 | [\hat{j}, \hat{x}] | 0 \rangle = -e^2 a^2 \langle 0 | \hat{H}_0 | 0 \rangle, \end{aligned}$$

where in the last step we have used the identity [see Eq. (4)]

$$\begin{aligned} [\hat{j}, \hat{x}] &= iea^2 \sum_{i, \sigma} (\hat{a}_{i, \sigma}^\dagger \hat{a}_{i+1, \sigma} + \hat{a}_{i, \sigma}^\dagger \hat{a}_{i-1, \sigma}), \\ &= -iea^2 \hat{H}_0. \end{aligned} \quad (16)$$

From the definition (6) of the effective mass, we see that Eq. (16) yields the sum rule (9).

The quantity $Z(\omega)$ was calculated numerically for $N=5$, $n=4$, and various values of the interaction constant $\mu = U/\epsilon_0$; the results are illustrated by the dotted lines in Fig. 2. To interpret these spectra, it is instructive to investigate the noninteracting case $\mu = 0$ in some detail. The one-electron wave functions which diagonalize the kinetic energy are easily seen to be

$$\psi_m(k) = \begin{cases} (\frac{2}{5})^{1/2} \sin(\frac{1}{6} \pi km) & (m=2, 4) \\ (\frac{2}{5})^{1/2} \cos(\frac{1}{6} \pi km) & (m=1, 3, 5) \end{cases} \quad (17)$$

with corresponding energies $-\epsilon_0 \cos \frac{1}{6} \pi m$. Here, k is a site index running from -2 to $+2$. Thus, the ground state of the "molecule" can be represented as in Fig. 3. Since the current operator is odd in k , the only allowed (dipole) transitions from occupied to excited states are $(m=1) \rightarrow (m=4)$ and $(m=2) \rightarrow (m=3 \text{ or } 5)$. The corresponding excitation energies are $\Delta E_{14} = \Delta E_{25} = 1.38\epsilon_0$ and $\Delta E_{23} = 0.5\epsilon_0$. These transitions are apparent in the spectrum shown in Fig. 2(a); since these are the only possible transitions, they must exhaust the sum rule (9). The spectrum of an *infinite* noninteracting

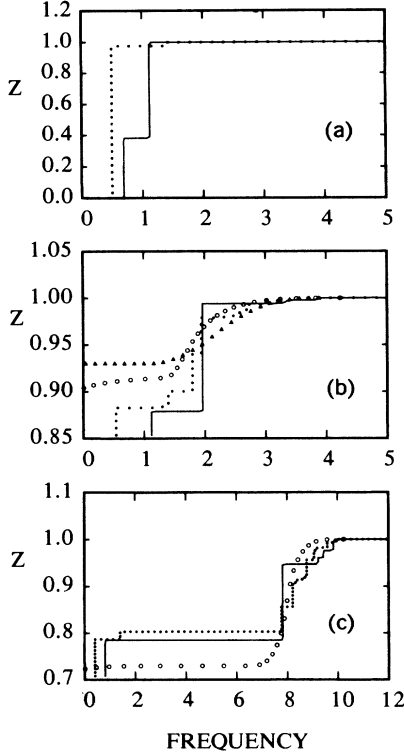


FIG. 2. Normalized, integrated conductivity as defined in Eq. (12) for a Hubbard system with $c=0.8$ electrons per atom and (a) $U=0$, (b) $U=\epsilon_0$, (c) $U=8\epsilon_0$. Continuous curves, five-atom ring; dots, five-atom linear chain; open circles, t -matrix approximation; triangles, memory-function approximation. Frequency is in units of ϵ_0 .

chain, on the other hand, would simply be a step function with a discontinuity at $\omega=0$. Thus, we can look at the finite chain spectrum as a coarse grained approximation to the infinite chain spectrum, with an energy resolution of order $2\epsilon_0/N$. As the interaction parameter μ increases, some of the low-frequency absorption is shifted to higher energy, which would correspond to a peak in the

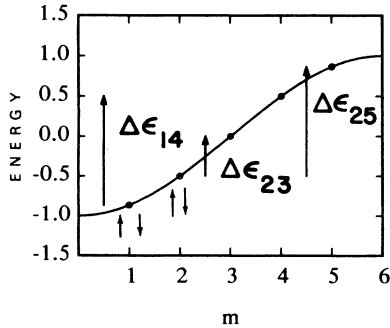


FIG. 3. Ground-state and optical transitions of a noninteracting five-atom linear chain.

real part of the conductivity. This absorption peak occurs at a frequency which increases with μ , and is roughly $U=\mu\epsilon_0$ when $\mu \gg 1$. It must therefore correspond to a transition in which the final state contains two electrons of opposite spin sitting on the same atom. In Sec. III, it will be shown that this transition involves a high-energy “bound state” which is responsible for most of the high-frequency absorption.

The model discussed above has a density of $c=0.8$ electron per site, which is a nearly half-filled system. In order to increase the number of sites and reduce the value of c , we have also calculated the function $Z(\omega)$ for rings of 5 and 7 sites. The advantage of working with a ring is that periodic boundary conditions can be imposed, and wave-vector conservation ensues. One can then restrict oneself to translation-invariant states, which reduces the dimension of the Hilbert space considerably. Although it is still possible to induce an electric field along the ring by changing the magnetic flux through it, the corresponding “conductivity” is related to the diamagnetic susceptibility of the system and does not satisfy the sum rule (9). Therefore, it is preferable to apply a uniform electric field; the coupling term in the Hamiltonian can again be calculated from Eq. (2), and is given by (c now denotes the speed of light)

$$\hat{H}_{A,r} = \left(\frac{A}{c}\right) \hat{j}_r + \frac{1}{2} \left(\frac{e}{c}\right)^2 A^2 a^2 (-\hat{H}_0) + \frac{\epsilon_0}{4} \left(\frac{e}{c}\right)^2 A^2 a^2 \sum_{k,\sigma} \cos\left(\frac{4\pi k}{N} + 2\psi\right) \times (\hat{a}_{k+1,\sigma}^\dagger \hat{a}_{k,\sigma} + \hat{a}_{k,\sigma}^\dagger \hat{a}_{k+1,\sigma}), \quad (18)$$

where the current operator is now

$$\hat{j}_r = iea \frac{\epsilon_0}{2^{1/2}} \sum_{k,\sigma} \cos\left(\frac{2\pi k}{N} + \psi\right) (\hat{a}_{k+1,\sigma}^\dagger \hat{a}_{k,\sigma} + \hat{a}_{k,\sigma}^\dagger \hat{a}_{k+1,\sigma}). \quad (19)$$

In these equations, ψ is a phase angle depending on the orientation of the electric field. The factor $2^{1/2}$ in the last equation provides a convenient normalization. The expectation value of the last term in Eq. (18) in the (translation-invariant) ground state is obviously zero, and the conductivity is again given by Eqs. (5)–(7), in which \hat{j} is replaced by \hat{j}_r . The sum rule (9) remains unchanged. Numerical results for rings of five atoms containing four electrons are shown in Fig. 2 (continuous lines), and are in good agreement with the results for the linear chain (dotted lines). In the noninteracting case $\mu=0$, the spacing between the one-electron energy levels is larger than in the linear case, which results in a poorer energy resolution. The locations

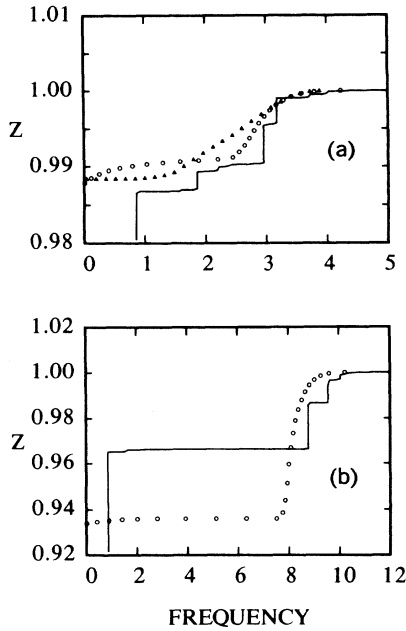


FIG. 4. Normalized, integrated conductivity as defined in Eq. (12) for a Hubbard system with $c = 0.571$ electrons per atom and (a) $U = \epsilon_0$, (b) $U = 8\epsilon_0$. Continuous curves, seven-atom ring; open circles, t -matrix approximation; triangles, memory-function approximation. Frequency is in units of ϵ_0 .

and strengths of the main absorption peaks, however, are in good agreement. This indicates that the high-frequency conductivity is relatively insensitive to the boundary conditions, even for $N = 5$. Figure 4 shows numerical results for rings of seven atoms. Note that this yields an electron density $c = 0.571$, which is close to the observed density of TTF-TCNQ.¹³ The comparison with the approximate theories of the infinite chain absorption will be carried out in Secs. III and IV.

III. T-MATRIX APPROACH

In the absence of interactions, \hat{j} commutes with the Hamiltonian and the commutator in Eq. (3) vanishes, so that there is no optical absorption and the dc conductivity is infinite. Thus, absorption processes must involve collisions between electrons. In a dilute system, collisions are rare and can be treated "one at a time." Let us therefore consider a system of two electrons having opposite spins and interacting via a Hubbard potential U . If the electrons are in a triplet state, the spatial wave function is antisymmetric and they do not interact. Hence, it will always be assumed that the colliding electrons are in a singlet state. The matrix elements of the two-particle Hamiltonian are

$$\begin{aligned} \langle k_1, k_2 | \hat{H} | k'_1, k'_2 \rangle = & -\epsilon_0 \delta_{k_1, k'_1} \delta_{k_2, k'_2} (\cos ak_1 + \cos ak_2) \\ & + (1/N) \delta_{k_1 + k_2, k'_1 + k'_2} U, \end{aligned} \quad (20)$$

where $|k_1, k_2\rangle$ and $|k'_1, k'_2\rangle$ denote normalized plane wave states. It is convenient to introduce the (dimensionless) "center of mass" and "relative" coordinates $q = \frac{1}{2}a(k_1 + k_2)$ and $\alpha = \frac{1}{2}a(k_1 - k_2)$, so that the kinetic energy of a state $|k_1, k_2\rangle$ takes the simple form $\epsilon_{q, \alpha} = -2\epsilon_0 \cos q \cos \alpha$. If we restrict q and α to the domain $0 < q < \pi$, $-\pi < \alpha < \pi$, q is a conserved quantity. Since we are interested in the singlet state, we limit ourselves to spatially symmetric wave functions. Hence we may further assume that $\alpha > 0$. To find the eigenstates of the two-particle Hamiltonian, we solve the Lippmann-Schwinger equation [a scattering eigenstate with initial quantum numbers q and α is denoted by $|q, \alpha\rangle$, while $|q, \alpha\rangle$ denotes a non-interacting eigenstate].

$$\begin{aligned} \langle q, \alpha' | q, \alpha \rangle = & \delta_{\alpha, \alpha'} + (2/N)U \\ & \times \sum_{\alpha'' > 0} \langle q, \alpha'' | q, \alpha \rangle / (\epsilon_{q, \alpha} - \epsilon_{q, \alpha''} - i\eta). \end{aligned} \quad (21)$$

This separable equation is immediately solved, with the result that

$$\langle q, \alpha' | q, \alpha \rangle = \delta_{\alpha, \alpha'} + \frac{(1/N)U f(q, \cos \alpha)}{(\epsilon_{q, \alpha} - \epsilon_{q, \alpha'} - i\eta)}, \quad (22)$$

where the "scattering amplitude" $f(q, \cos \alpha)$ is given by

$$1/f(q, \cos \alpha) = 1 + U/(2i\epsilon_0 |\sin \alpha \cos q|). \quad (23)$$

In addition to the scattering states, the Hamiltonian (20) has a bound state $|q, b\rangle$ for arbitrary q . For the repulsive interaction $U > 0$ considered here, the bound state lies *above* the highest band energy $2\epsilon_0$. The ability of a repulsive potential to bind electrons from a tight-binding band was first noted in Ref. 14 in the case of an impurity. The equation for the bound state is analogous to (21) without the inhomogeneous term $\delta_{\alpha, \alpha'}$; the normalized bound-state wave function is found to be

$$\langle q, \alpha | q, b \rangle = \frac{(2U^3/\epsilon_q)^{1/2}}{\epsilon_{q, \alpha} - \epsilon_q}, \quad (24)$$

where the bound state energy ϵ_q is given by

$$\epsilon_q = (U^2 + 4\epsilon_0^2 \cos^2 q)^{1/2}. \quad (25)$$

We now use these results to calculate the correlation function χ for a two-electron system in an eigenstate $|q, \alpha\rangle$, which we will denote by $\chi(q, \alpha, \omega)$. We will then approximate the correlation function for the dilute Hubbard chain by averaging $\chi(q, \alpha, \omega)$ over all the pairs of electrons present in

the system according to

$$\chi(\omega) = \sum_{k_1 > k_2} \chi(\frac{1}{2}a(k_1 + k_2), \frac{1}{2}a(k_1 - k_2), \omega) n_{k_1, k_2}, \quad (26)$$

where n_{k_1, k_2} is the joint distribution function for a

pair of electrons in a singlet state:

$$n_{k_1, k_2} = \langle \hat{S}_{k_1, k_2}^\dagger \hat{S}_{k_1, k_2} \rangle, \quad (27)$$

$$\hat{S}_{k_1, k_2} = \frac{1}{2^{1/2}} (\hat{a}_{k_1 \uparrow} \hat{a}_{k_2 \downarrow} - \hat{a}_{k_1 \downarrow} \hat{a}_{k_2 \uparrow}).$$

Writing $\chi = \chi' + i\chi''$, one finds from Eq. (7)

$$\chi''(q, \alpha, \omega) = \pi \sum_{\alpha' > 0} |(q, \alpha | \hat{j} | q, \alpha')|^2 [\delta(\omega + \epsilon_{q, \alpha} - \epsilon_{q, \alpha'}) - \delta(\omega - \epsilon_{q, \alpha} + \epsilon_{q, \alpha'})]$$

$$+ \pi |(q, \alpha | \hat{j} | q, b)|^2 [\delta(\omega + \epsilon_{q, \alpha} - \epsilon_q) - \delta(\omega - \epsilon_{q, \alpha} + \epsilon_q)]. \quad (28)$$

Note that this expression is very similar to that obtained for interband absorption in a semiconductor. The main difference is, of course, that in the present case the optical transitions occur between two- rather than one-particle states. The first term contains the effect of transitions to continuum (scattering) states, and the second term arises from transitions to the bound state. Using the above expressions for the eigenstates of the two-electron Hamiltonian, the matrix elements of the current operator are easily found to be (assuming $\alpha \neq \alpha'$)

$$(q, \alpha | \hat{j} | q, \alpha') = 2a(U/N) \tan q f(q, \cos \alpha') f^*(q, \cos \alpha),$$

$$(q, \alpha | \hat{j} | q, b) = (2U^3 a^2 / \epsilon_q N)^{1/2} f^*(q, \cos \alpha) \tan q. \quad (29)$$

Substituting these matrix elements in Eq. (28) for the correlation function, one finds after some algebra

$$\chi''(q, \alpha, \omega) = 2(U/N)a^2 \tan^2 q |f(q, \cos \alpha)|^2 F(q, \alpha, \omega)$$

$$+ 2\pi(U^3 a^2 / \epsilon_q N) |f(q, \cos \alpha)|^2 \tan^2 q$$

$$\times [\delta(\omega + \epsilon_{q, \alpha} - \epsilon_q) - \delta(\omega - \epsilon_{q, \alpha} + \epsilon_q)], \quad (30)$$

where $[\Theta(x) = 0 \text{ if } x < 0, 1 \text{ if } x > 0]$

$$F(q, \alpha, \omega) = \Theta(4\epsilon_0^2 \cos^2 q - (\omega + \epsilon_{q, \alpha})^2)$$

$$\times \text{Im} f\left(q, \frac{\omega + \epsilon_{q, \alpha}}{2\epsilon_0 \cos q}\right)$$

$$- \Theta(4\epsilon_0^2 \cos^2 q - (\omega - \epsilon_{q, \alpha})^2)$$

$$\times \text{Im} f\left(q, \frac{\epsilon_{q, \alpha} - \omega}{2\epsilon_0 \cos q}\right). \quad (31)$$

The first term in the right-hand side of Eq. (30) arises from transitions into continuum two-particle states. This term agrees with the result of Lyo and Holstein.⁵ The second term accounts for transitions into the bound state. Since q, α , and k_F

are of order c and since $f \sim |\sin \alpha| \sim c$ in the dilute limit, both terms are of order c^4 . After integrating over q and α to obtain the real part of the conductivity, these terms are of order c^6 and c^5 respectively (the δ function in the bound state term removes one power of c). This result can be understood by noting that in the dilute limit, electrons sit near the bottom of the band and the dispersion relation is approximately parabolic, leading to momentum conservation and the vanishing of the absorption.

To obtain the current-current correlation function of the system, hence the conductivity, it remains to sum Eq. (31) over the momenta of the incoming particles as specified by Eq. (26). This was done numerically. The open circles in Figs. 2 and 4 show the results for the normalized integrated conductivity $Z(\omega)$, defined in Eq. (12). The corresponding electron densities are $c = \frac{4}{5}$ and $c = \frac{4}{7}$ respectively. In the case $\mu = 1$, we have neglected the effect of correlation in the effective mass and in the two-particle distribution function. Thus, we set

$$1/m^* = a^2 \epsilon_0 \frac{\sin(\pi c/2)}{\pi c/2},$$

$$n_{k_1, k_2} = \begin{cases} 1 & \text{if } |k_1|, |k_2| < k_F, \\ 0 & \text{otherwise } (\mu \text{ small}). \end{cases} \quad (32)$$

In the strongly interacting case, however, the oscillator strength of the main absorption peak was found to be several times smaller than found numerically for finite chains and rings. This is clearly due to correlation effects, which tend to shift some of the weight of the two-particle distribution function to higher values of the momenta. Since the response function (29) increases rapidly with the reduced momenta q and α , this enhances the absorption. As a crude way to include such effects, we assumed that the particle momenta were uniformly distributed between $-2k_F$ and $+2k_F$.

Thus, we set

$$\frac{1}{m^*} = a^2 \epsilon_0 \frac{\sin(\pi c)}{\pi c},$$

$$n_{k_1 k_2} = \begin{cases} \frac{1}{4} & \text{if } |k_1|, |k_2| < 2k_F \\ 0 & \text{otherwise } (\mu \text{ large}). \end{cases} \quad (33)$$

This ansatz can be justified as follows. It is easily seen that, in the limit $\mu \rightarrow \infty$, the spatial part of the ground-state wave function of the one-dimensional Hubbard model is identical with that of a system of noninteracting, spinless fermions within a factor ± 1 . This factor arises because the spinless fermion wave function is odd under the interchange of two spatial coordinates, while the wave function of the Hubbard model is odd under the simultaneous interchange of spatial and spin coordinates. If we concentrate on a pair of neighboring electrons in a singlet state, therefore, the full spatial wave function must behave as a sum of terms of the form $C |\sin \frac{1}{2} (k_1 - k_2)(x_1 - x_2)| \times \exp[i \frac{1}{2} (k_1 + k_2)(x_1 + x_2)]$, where x_1, x_2 denote the coordinates of the two electrons and the two momenta k_1, k_2 are uniformly distributed between $-2k_F$ and $+2k_F$; C is a constant which depends on the remaining coordinates x_3, \dots . Together with the observation that only short-range correlations should be important, we are naturally led to the above ansatz.

With Eqs. (32) and (33), the t -matrix predictions for $Z(\omega)$ are in good agreement with the numerical spectra. The largest discrepancy arises in the case $c = 0.571$, $\mu = 8$ as shown in Fig. 4 (b). We checked that the discrepancy decreases with increasing U . This confirms our interpretation of the main absorption peak in terms of a bound state consisting of two electrons sitting at the same site. Figure 5 shows the dimensionless conductivity σ^* , defined by

$$\sigma^*(\omega) = \frac{2}{\pi} \frac{m^* \epsilon_0}{n e^2} \sigma'(\omega) \quad (34)$$

in the same approximation. Clearly, it is only in the weak coupling limit $\mu \ll 1$ that continuum transitions (open circles) contribute significantly to the absorption; for $\mu \sim 1$ most of the absorption is due to the bound state. It must be noted that the relatively large contribution of continuum transitions to the low-frequency absorption is a spurious effect, due to our neglect of the Pauli principle in the summation over final states in Eq. (28). Restricting the sum over α' to unoccupied states would suppress this contribution. However, this correction is formally of higher order in the electron density c . Since the contribution of continuum transitions to the t -matrix conductivity is small when $\mu \sim 1$, we did not include this refinement in the t -matrix calculation.

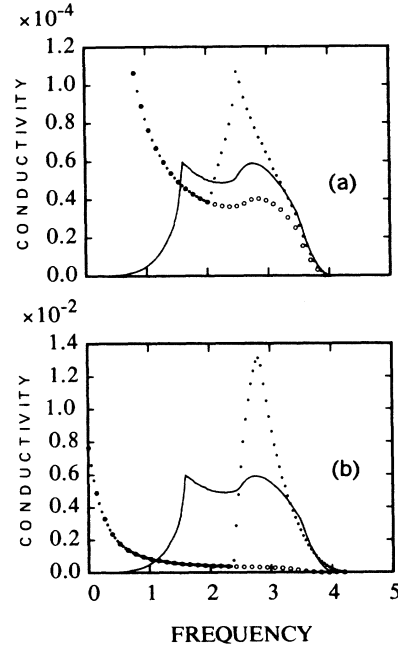


FIG. 5. Dimensionless conductivity [Eq. (34)] calculated in the t -matrix approximation (dotted curves) and in the memory function approximation (continuous curves) for $c = 0.571$ electrons per atom and (a) $U = 0.1 \epsilon_0$, (b) $U = \epsilon_0$. The open circles represent the contribution of transitions into the continuum to the t -matrix conductivity. Frequency is in units of ϵ_0 .

IV. MEMORY-FUNCTION APPROACH

In this section, we will use the memory-function approach of Götze and Wölfle to calculate the conductivity of an infinite Hubbard chain in the weak coupling limit (i.e., $\mu \rightarrow 0$). We begin with an outline of the formalism. The memory function $M(\omega)$ is defined in terms of the conductivity by the formula⁶

$$\sigma(\omega) = i(n e^2 / m^*) [1 / (\omega + M(\omega))]. \quad (35)$$

In particular, $M(\omega) = i/\tau$ in the Drude approximation. Thus, M can be interpreted as a frequency-dependent generalization of the relaxation rate. Just as the conductivity, the memory function is analytic in the upper frequency half-plane. The basic assumption of the theory is that M is a well-behaved function of ω and of the strength of the interaction. One can then expand Eq. (35) at high frequency:

$$\sigma(\omega) = i(n e^2 / m^*) [1/\omega - M(\omega)/\omega^2 + \dots]. \quad (36)$$

Thus, $M(\omega)$ is simply obtained by expanding the conductivity to leading order in the interaction. Extrapolation to all frequencies yields the memory-function approximation. Although we have made no effort toward rigor, it can be shown that this approximation is actually the first term of a con-

tinued fraction expansion of the conductivity. In the present context, we view the memory-function approximation as the simplest approximation which satisfies the sum rule (9) and reduces to perturbation theory at high frequency.

From Eqs. (36) and (7), one finds after some algebra that the memory function can be written as

$$M(\omega) = \frac{m^*}{ne^2\omega} [\pi(\omega) - \pi(0)], \tag{37}$$

where the correlation function π is given by

$$\pi(\omega) = i \int_0^\infty dt e^{i\omega t} \langle [\hat{F}(t), \hat{F}(0)] \rangle. \tag{38}$$

Here, the "force operator" \hat{F} is defined according to

$$\hat{F} = -i[\hat{j}, \hat{H}]. \tag{39}$$

It is now straightforward to calculate the correlation function (37) to leading order in the interaction U . The force operator (38) is simply

$$2iea\epsilon_0 \frac{U}{N} \sum_{k,p,q} \hat{a}_{k+q}^\dagger \hat{a}_{k+q} \hat{a}_{p-q}^\dagger \hat{a}_p \times \sin \frac{1}{2} a(k+p) \{ \cos a[\frac{1}{2}(k-p)+q] - \cos \frac{1}{2} a(k-p) \} \tag{40}$$

so that, to leading order in U , the average in Eq. (38) can be taken in a noninteracting system. The corresponding diagram is shown in Fig. 6. Using the standard rules of perturbation theory, one finds ($M = M' + iM''$)

$$M''(\omega) = \frac{\pi U_a^2}{2\omega\epsilon_0 \sin \pi c/2} \int_0^{2\pi/a} \frac{dq}{2\pi} \int_0^\omega \frac{d\Omega}{\pi} [2\chi_2(q, \Omega)\chi_0(-q, \omega - \Omega) + 2\chi_1(q, \Omega)\chi_1(-q, \omega - \Omega)], \tag{41}$$

where

$$\chi_n(q, \omega) = \int_0^{2\pi/a} \frac{dp}{2\pi} \delta(\epsilon_p - \epsilon_{p-q} - \omega) \times (n_{p-q} - n_p)(v_p - v_{p-q})^n. \tag{42}$$

Here $\epsilon_p = -\epsilon_0 \cos ap$ is the electron energy, $v_p = a\epsilon_0 \sin ap$ is the velocity, and n_p is the zero-temperature occupation number, $n_p = 1$ if $|p| < k_F = \pi c/2a, = 0$ otherwise. The two-dimensional integral in Eq. (42) is easily evaluated numerically, and the real part M' of the memory function is obtained by using a dispersion relation.

The results for the normalized integrated conductivity $Z(\omega)$ [Eq. (12)] are shown in Figs. 2 and 4, and those for the dimensionless conductivity σ^* [Eq. (34)] in Fig. 5. The absorption predicted by the memory function approximation is of the correct order of magnitude for $\mu = 1$. In the weak coupling limit $\mu \ll 1$, one would expect the t -matrix and memory function approaches to yield similar

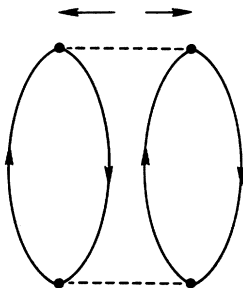


FIG. 6. Feynman diagram for the correlation function π defined in Eq. (38).

results. Figure 5 shows that this is indeed the case for $\mu = 0.1$, although (i) the bound-state contribution to the t -matrix is still substantial even though it is formally of order μ^3 [see Eq. (30)], and (ii) the t -matrix absorption is too large at low frequency, as discussed in the previous section. The peak around $\omega = 1.6\epsilon_0$ in the memory function approximation curves arises from a singularity in the integrand of the expression (41) for the memory function. This is illustrated in Fig. 7, which shows the domains in the (q, Ω) plane where the susceptibilities $\chi_m(q, \Omega)$ and $\chi_n(-q, \omega - \Omega)$ are nonvanishing [see Eq. (42)].

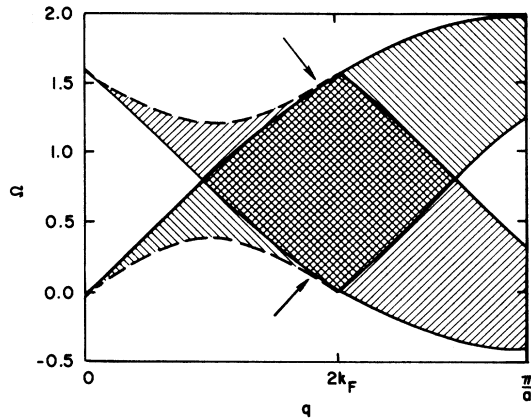


FIG. 7. Domains in which the factors $\chi_m(q, \Omega)$ and $\chi_n(-q, 1.58\epsilon_0 - \Omega)$ in Eq. (41) are different from zero. The arrows indicate the regions of critical contact, and the dashed lines are the boundaries imposed by the Pauli principle. Ω is in units of ϵ_0 .

For certain values of ω , the boundaries of these domains are in critical contact; such values of ω will correspond to singularities in the slope of the memory function, provided that the velocity factor in Eq. (42) does not vanish at the point of critical contact. As discussed in the previous section, our t -matrix approximation neglects the Pauli principle in the summation over final states. The domains shown in Fig. 7 are then enlarged, and the points of critical contact disappear. This explains why the t -matrix curve goes on increasing below the value $\omega = 1.58\epsilon_0$.

Figure 5(b) shows the dimensionless conductivity for $\mu = 1$, and it is clear that the apparent order-of-magnitude agreement between the memory-function approximation and the numerical spectra is due to a fortuitous cancellation of two effects. On the one hand, the memory-function approximation neglects the important bound state contribution. On the other hand, the Born approximation used in the memory-function approximation overestimates the cross-section for scattering into continuum states. In the strong coupling limit, the second effect is stronger and the memory-function approximation breaks down completely.

V. CONCLUSION

The numerical results presented in this paper substantiate the claim made in the introduction that the optical absorption of the one-dimensional Hubbard model with an electron density comparable to that of TTF-TCNQ is small. Thus, for $U = 8\epsilon_0$, we find that the main absorption peak exhausts about 4% of the sum rule. Moreover, within the "energy resolution" $\Delta\omega \sim \epsilon_0$ of our finite chain and ring calculations, we find no low-frequency anomaly in the spectrum. In the case of KCP, we find that the absorption is even smaller; for instance, setting $c = 0.3$ and $U = \epsilon_0$, the t -matrix approximation yields a normalized conductivity $\sigma^*(\omega)$ which is less than 2×10^{-3} for $\omega > 0$. On the positive side, we have shown that the t -matrix approximation is in good agreement with the numerical spectra of finite chains and rings. This indicates that the short-range correlations which are important for the optical conductivity are properly taken into account by that approximation. It also suggests that a similar approximation may be useful in the study of more sophisticated models including both the electron-electron and the electron-phonon interactions.

¹J. B. Torrance, B. A. Scott, and F. B. Kaufman, *Solid State Commun.* **17**, 1369 (1975).

²P. F. Williams, M. A. Butler, D. L. Rousseau, and A. N. Bloch, *Phys. Rev. B* **10**, 1109 (1974).

³R. P. Messmer and D. R. Salahub, *Phys. Rev. Lett.* **35**, 533 (1975).

⁴S. K. Lyo, *Phys. Rev. B* **14**, 2335 (1976).

⁵S. K. Lyo and T. Holstein, *Phys. Rev. B* **14**, 5137 (1976).

⁶W. Götze and P. Wölfle, *Phys. Rev. B* **6**, 1226 (1972).

⁷S. Suhai, *J. Phys. C* **9**, 3073 (1976).

⁸B. N. Cox, M. A. Coulthard, and P. Lloyd, *J. Phys. F* **4**, 807 (1974).

⁹A. Luther and I. Peschel, *Phys. Rev. B* **9**, 2911 (1974).

¹⁰Yu. A. Bychkov, L. P. Gor'kov, and I. E. Dzyaloshinskii, *Sov. Phys.-JETP* **23**, 489 (1966) [*Zh. Eksp. Teor. Fiz.* **50**, 738 (1966)].

¹¹D. C. Mattis and E. H. Lieb, *J. Math. Phys.* **6**, 304 (1965).

¹²I. Sadakata and E. Hanamura, *J. Phys. Soc. Jpn.* **34**, 882 (1973).

¹³R. Comes, S. N. Shapiro, G. Shirane, A. F. Garito, and A. J. Heeger, *Phys. Rev. Lett.* **35**, 1518 (1975).

¹⁴G. F. Koster and J. C. Slater, *Phys. Rev.* **95**, 1167 (1954).